THE JOURNAL OF PHYSICAL CHEMISTRY B

ARTICLE

pubs.acs.org/JPCB

Sequence-Specific Mg^{2+}—DNA Interactions: A Molecular Dynamics Simulation Study

Weifeng Li,[†,‡] Lars Nordenskiöld,[‡] and Yuguang Mu*[,‡]

[†]School of Physical and Mathematical Sciences, 21 Nanyang Link, and [‡]School of Biological Sciences, 60 Nanyang Drive, Nanyang Technological University, Singapore

ABSTRACT: The effects of Mg^{2+} ions, in comparison with Na^+ ions, on DNA structure and conformational dynamics were studied by molecular dynamics simulations. Mg^{2+} ions, with a stable hydration shell consisting of six water molecules, interact with DNA mainly through hydrogen bond interactions, which are sensitive to the local environment. Mg^{2+} ions were found at the phosphate backbone and selectively in the major groove of G·C bases. The sequence-dependent specificity is of electrostatic nature and not caused by steric constraints. The adjacent N7 and O6 atoms at the guanine base create a negative potential environment and act as hydrogen bond acceptor for hydrated Mg^{2+} ions, while the positively charged H atoms on the N6 amino group of adenine base repel the hydrated Mg^{2+}. The binding of Mg^{2+} makes the DNA duplex more rigid compared to the Na—DNA system, as demonstrated by reduced conformational entropy and restricted local bending motion. The sequence-specific interaction between Mg^{2+} and DNA molecules provides a hint into a rich condensation behavior of DNA in the sequence context by Mg^{2+} ions.

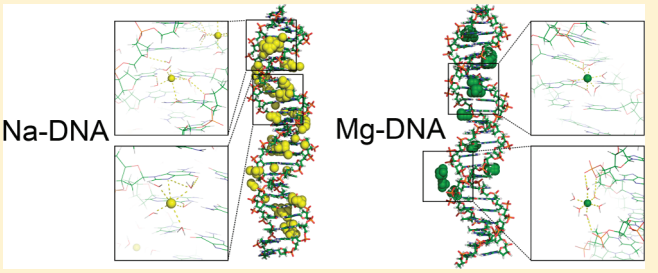

1. INTRODUCTION

Due to the polyelectrolyte nature of nucleic acids, their structures and functions are sensitively correlated with the "counterion atmosphere".[1−5] Since the DNA backbone is negatively charged, the close contact between DNA duplexes is strongly repulsive. The counterion atmosphere around DNA plays the role of electrostatic screening to reduce the repulsion. The direct evidence of intimate interactions between cations and nucleic acids came from crystal structures where dehydrated sodium ions (Na^+) were found in the minor groove of DNA.[6,7] Compared with monovalent ions, divalent ions (like Mg^{2+}) have stronger interactions with nucleic acids[8,9] and are critical in genomic DNA folding.[10] DNA structure and dynamics are fundamental in keeping genome stability.[11]

The ion—DNA interactions are highly dynamic, which makes it difficult for experiments to provide a microscopic tempo-spatial description. On the other hand, computer molecular dynamics (MD) simulations based on potential energy functions are effective in deciphering the interaction nature of ions and water with DNA.[12−16] The advantage of MD simulations is that the simulations can describe not only how ions screen the electrostatic interaction, i.e., the "passive" screening effects, but also the "active" effects of ions on DNA dynamics at the atomic details. So far most studies were targeted on monovalent ions, such as Na^+ and K^+ ions;[17−21] for divalent ions, such as Mg^{2+} ions, their detailed interacting picture with DNA obtained from MD simulations is scarcely documented.[13,22]

One reason for limited MD studies of DNA in the presence of Mg^{2+} is that Mg^{2+} ions could form polar covalent bonds with oxygen atoms on the phosphate group of DNA. The chemical polar bond formation process is beyond the scope of classic MD simulations. For most Mg^{2+} ions there was no direct evidence of polar bond formation with the DNA duplex.[23] As a result, directly polar bonded, or "chelated", Mg^{2+} ions only constitute a small number of observed ions.[24] In fact, Mg^{2+} ions have a closed shell electron structure and a stable water coordination shell in solvent. They interact with DNA primarily through electrostatic and van der Waals dispersion forces. These fully hydrated mobile ions contribute a dominant role in stabilization of RNA structure resolved by thermodynamic analysis.[25]

Based on the above considerations, we performed classical MD simulations in the presence of explicit water and counterions, to explore the atomic interaction picture of Mg^{2+} with the DNA duplex and the effects of Mg^{2+} ions on the DNA structure and dynamics, in comparison with the DNA system in the presence of Na^+ ions.

2. SIMULATION DETAILS

A. System Setup. Two different setups and several DNA models were employed: In the first setup, one isolated double-stranded 23-mer DNA (GGCGGCGGCGCGGCGTTTTTTGG)[26] was solvated in a $10 \times 10 \times 10\ nm^3$ water box. Two simulations in different electrolytes have been performed: (1) one simulation contained 67 Na^+, 23 Cl^-, and 32 007 water (named as Na—DNA for short); (2)

Received: June 4, 2011
Revised: September 26, 2011
Published: October 30, 2011

Table 1. Simulation System Setups

	simulation box content					
system name	DNA	Na^+	Mg^{2+}	Cl^-	H_2O	cation's molar concentration (M)
Na−DNA	23-mer DNA	67	0	23	32007	0.083
Na−pGG	$dG_{10}\cdot dC_{10}$	20	0	0	4314	0.165
Na−pGC	$d(GC)_5\cdot d(CG)_5$	20	0	0	4323	0.177
Na−pAA	$dA_{10}\cdot dT_{10}$	20	0	0	4309	0.195
Na−pAT	$d(AT)_5\cdot d(TA)_5$	20	0	0	4317	0.166
Mg−DNA	23-mer DNA	29	19	23	31980	0.041 (Na) 0.017 (Mg)
Mg−pGG	$dG_{10}\cdot dC_{10}$	0	20	20	4314	0.185
Mg−pGC	$d(GC)_5\cdot d(CG)_5$	0	20	20	4323	0.194
Mg−pAA	$dA_{10}\cdot dT_{10}$	0	20	20	4309	0.155
Mg−pAT	$d(AT)_5\cdot d(TA)_5$	0	20	20	4317	0.173

Table 2. CHARMM Force Field Parameters of Na^+ and Mg^{2+} Used in Our Simulations

	mass	σ (nm)	ε (kJ/mol)
Na^+	22.98977	2.42992×10^{-1}	1.962296×10^{-1}
Mg^{2+}	24.30000	2.11143×10^{-1}	6.27600×10^{-2}

the other simulation contained 29 Na^+, 19 Mg^{2+}, 23 Cl^-, and 31 980 water (named as Mg−DNA,).

In the second setup, periodic DNA double strands with different sequences were studied. The system contained one double-stranded 10-mer DNA solvated in a $7 \times 7 \times \sin 60° \times 3.4$ nm^3 hexagonal water box. DNA duplex is infinite as each strand is covalently bonded to its image over the periodic boundary at the z direction. In order to compare the sequence-specific ions−DNA attraction, four periodic-DNAs (pDNA for short in the later discussions) with different sequences were simulated: (1) polyG·polyC, named as pGG (periodic polyG), (2) polyA·polyT, named as pAA, (3) poly[dGdC]·poly[dCdG], named as pGC (periodic poly[dGdC]), and (4) poly[dAdT]·poly[dTdA], named as pAT. Other than DNA, the simulation box contains 4000 water molecules, 20 Mg^{2+}, and 10 Cl^- (in the Mg−pDNA case) or 20 Na^+ (in the Na−pDNA case).

The molar concentration of the ions was evaluated from the solution far from the DNA atoms.[27] The ion concentration, together with the system contents of all the simulation systems, is listed in Table 1.

B. Simulation Protocol. For DNA, we have used the latest parmbsc0 force field.[28] The initial coordinates of DNA models were B-form generated with nucleic acid builder (nab).[29] For Na^+, Cl^-, and Mg^{2+}, the CHARMM parameters optimized by Roux and co-workers[30] were used and are listed in Table 2. For water, we used the TIP3P[31] water model. All simulations were carried out using the GROMACS program version 4.0.3.[32] The systems were first minimized for 1000 steps followed by a preequilibration of 100 ps with the atoms of DNA fixed. Data production simulations were performed for 100 ns for all our models. All the simulations were performed within the NPT ensemble (300 K, 1 atm). SHAKE constrains[33] were applied to all bonds involving hydrogen atoms. van der Waals interactions were considered with a distance cutoff of 10 Å. Electrostatic interactions were treated using the particle mesh Ewald (PME) algorithm.[34,35] The movement integration time was 2 fs. The nonbonded interaction pair list was updated every 10 fs.

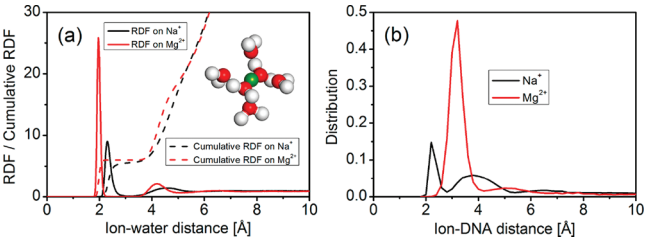

Figure 1. Radial distribution function (solid line) of water oxygen and cumulative number of waters (dashed line) around Na^+ (black-colored) and Mg^{2+} (red-colored) ions. The inset is a snapshot of the spatial configuration of six water molecules bounded to Mg^{2+} (a). Distribution of ion−DNA distance (b).

C. PCA Analysis and Conformational Entropy. Principal component analysis (PCA) is an efficient method to represent the conformational dynamics of a $3N$-dimensional system in terms of a few "principal" components.[36] The basic idea is that the internal motions are correlating and represented by the covariance matrix. By diagonalizing the matrix, we obtain $3N$ eigenvectors and eigenvalues, which are ranked in descending order; that is, number 1 represents the largest eigenvalue. The eigenvectors and eigenvalues yield the modes of collective motions and their amplitudes.

The conformational entropy is calculated by the method introduced by J. Schlitter.[37] It is based on the approximation that each degree of freedom can be represented by a quasi-harmonic oscillator whose vibration frequency can be estimated by the PCA analysis. The conformational entropy is a good parameter to describe the global dynamics of DNA, where lower conformational entropy corresponds to more rigid DNA having lower amplitudes of motion.

3. RESULTS AND DISCUSSION

A. Solvation Structure of Free Ions. First, we investigate the solvation patterns of Mg^{2+} and Na^+. The radial distribution function (RDF) of water oxygen atoms (OW) around the two cations are shown in Figure 1a (solid line). Clearly, there is a distinct first solvation shell (FSS) at a distance around 2 Å for

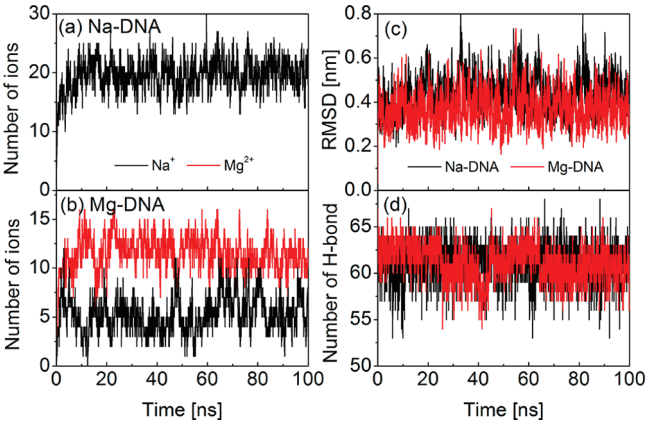

Figure 2. Time evolution of cation number on DNA surface: Na^+ ions in Na−DNA system (a); Na^+ (black line) and Mg^{2+} ions (red line) in Mg−DNA system (b). Time evolutions of root-mean-squared deviation (rmsd) of DNA in two simulations with respect to a reference structure of a standard B-DNA (c). Number of Watson−Crick hydrogen bonds (H-bond) in two simulations (d).

Mg^{2+} (red solid line) which is consistent with the findings of X-ray diffraction studies.[38] The second solvation shell (SSS) near 4.3 Å is weak. The dashed line in this figure gives the cumulative number of water molecules inside the first solvation shell. It is clear that six water molecules constitute the FSS of Mg^{2+}. One configuration of Mg^{2+} with bound water molecules is shown in the inset: six water molecules form an octahedral shape with all hydrogen atoms pointing outward, so that the Mg^{2+} + $6H_2O$ complex can function as hydrogen bond donors. The six surrounding water molecules are found to be very stable and did not exchange with bulk water during the 100 ns simulations. The nuclear magnetic resonance study showed that the mean residence time of water molecules bound to Mg^{2+} is 1.5 μs.[39]

For Na^+, the FSS (black solid line) is around 2.3 Å which is close to the value obtained from a study using recently optimized Na^+ parameters.[40] Although there are also six waters constituting the first solvation shell of Na^+, the height of the peak is left-shifted and reduced to one-third of that of Mg^{2+}. This means that the coordination sphere of Na^+ is relatively loose and less stable than that of Mg^{2+}, because of the weaker electrostatic attractions from monovalent Na^+. This coordination difference between Na^+ and Mg^{2+} will affect their interactions with DNA, which will be discussed later.

B. Results of Isolated DNA Model. *Ion−DNA Binding Pattern.* The distinct FSS of Mg^{2+} and Na^+ ions will affect their binding patterns when encountering the DNA surface. The cation binding behavior was monitored through calculation of the minimal distance between each Na^+/Mg^{2+} ion and the atoms of DNA (ion−DNA distance). The distributions of the ion−DNA distance are shown in Figure 1b. For Na^+ ions, there are two favorable binding positions: one is around 2.2 Å and the other is 4 Å from the DNA surface. The small distance of the former position means that Na^+ ions form direct contacts with DNA by discarding some water in its FSS. For the latter position, a Na^+ ion interacts with DNA through its FSS. For Mg^{2+} ions, there is only one obvious bound distance at 4 Å. Thus, Mg^{2+} can only interact with DNA through its FSS. This is not surprising because the FSS of Mg^{2+} is more stable than that of Na^+. When the distance is larger than 5 Å, the ion distribution curve is featureless. This indicates that beyond 5 Å the ions are almost free and there is no obvious binding behavior.

Charge Neutralization of the DNA. Cations will accumulate in the vicinity of DNA because of the Coulombic attraction. We have monitored the time evolution of bound ions on DNA as shown in Figure 2a and b. The definition of "bound ions" is made solely from a structural point of view. Based on the distribution function in Figure 1b, any ion is supposed to be bound, if the ion−DNA distance is less than 5 Å. For the Na−DNA system (Figure 2a), in the beginning of the simulation, the positions of the ions were assigned randomly in the water box, and there were only ~5 Na^+ bound to DNA. As the simulation went on, more Na^+ ions were approaching the DNA surface. At t = 10 ns, the number reached a plateau of around 20. During the rest of the simulation the number of Na^+ was nearly constant, albeit with considerable fluctuations. For the Mg−DNA system the interaction picture is shown in Figure 2b. After a 10 ns simulation, the number of bound Mg^{2+} increased to a plateau around 12. At the same time, the number of Na^+ was reduced to a value around 5. Evidently, Mg^{2+} ions are stronger competitors to the DNA surface than Na^+ ions.

An important role of the counterions is to neutralize the negative charge of the phosphate groups. The close contacts of the bound ions with DNA render their neutralizing effects to full strength. The neutralization fraction of DNA charge can be defined as

$$r = \sum_i z_i \times N_i^{\mathrm{b}} / Q_{\mathrm{dna}}$$

where z_i, N_i^{b}, and Q_{dna} are the valence, the number of bound ions of species i, and the charge of DNA, respectively. The average r value for the DNA duplex (discarding the two terminal base pairs) is calculated to be 50% (Na−DNA) and 71% (Mg−DNA), respectively.

DNA Double Helix Stability. The structural stability of the DNA double helix was checked through calculating the time evolution of the root-mean-squared deviation (rmsd) with respect to a standard B-form DNA (Figure 2c) and the number of Watson−Crick hydrogen bonds (H-bond) (Figure 2d). During both simulations of Na−DNA and Mg−DNA, the DNA structures are stable. The rmsd of the Mg−DNA case is slightly smaller than that of the Na−DNA case. The H-bonds are very well maintained and less affected by the electrolyte environment.

Counterion Clouds around DNA. Inspection of the spatial binding map, i.e., probability density of ions around the DNA, gives us a detailed global view of ion−DNA interaction. The simulation box was divided into three-dimensional grids with grid length of 1 Å, and the occupancy of ions for each grid was calculated. The yellow and green balls as shown in Figure 3 represent the grids with ion density >10 M for Na^+ in the Na−DNA case and >5 M for Mg^{2+} in the Mg−DNA case, respectively. For the Na−DNA system, Na^+ ions can occupy the minor groove of DNA in a nonspecific and diffusive way. As shown in Figure 3a, one Na^+ with five coordinated water molecules goes deep into the minor groove. The minor groove of G·C base has three H-bond acceptors: oxygen atoms (O4′) of the 2-deoxyribose sugar and O2/N3 atoms of the base pairs. In the major groove of G·C base, N7 and O6 of guanine base serve as hydrogen bond acceptors. We found that Na^+ can also lose several coordinated water molecules and form direct electrostatic interactions with these negative charged atoms. As shown in Figure 3b, the distance between Na^+ and the N7 atom is 2.82 Å, which is a direct contact.

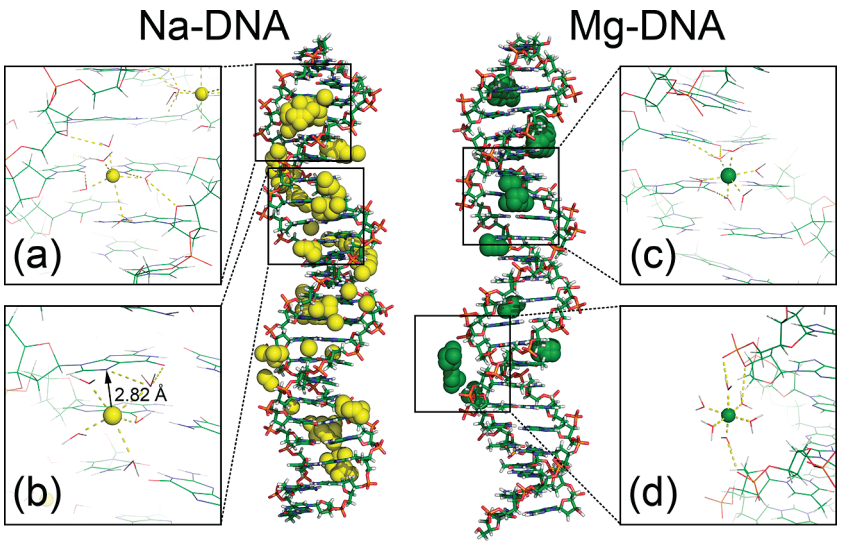

Figure 3. Stereoviews of counterions binding map around DNA duplex. The left side represents the Na−DNA system: Na^+ in minor groove (a), Na^+ in major groove (b). The right side represents the Mg−DNA system: Mg^{2+} in major groove (c); Mg^{2+} on phosphate group at A-tract region (d).

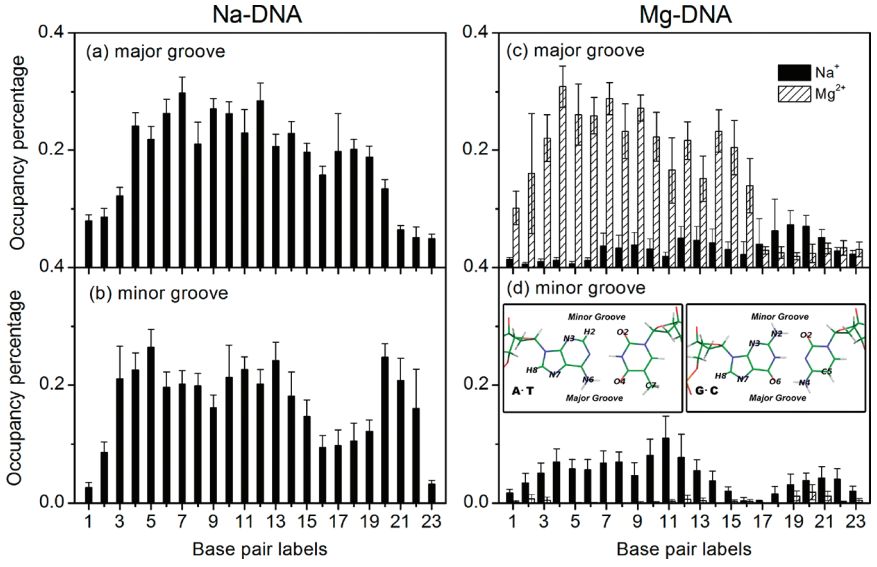

Figure 4. Number of bound ions projected on each base pair. The *x* axis indicates base pair sequence number (a−d). Base pair atoms used to define bounded ions in the major groove and minor groove are shown in the inset of (d).

For the Mg−DNA system, one distinct feature is that the hydrated Mg^{2+} cannot penetrate into the minor groove due to the reason that the $Mg^{2+} + 6H_2O$ complex is too big in size for the minor groove to accommodate it. Mg^{2+} only appears near the major groove of the GC-rich segment (Figure 3c). Most of the bound Mg^{2+} ions exist near the phosphate group because the phosphate groups are highly negatively charged. We also observed that at the A-tract segment (base 16−21) of Mg−DNA, some Mg^{2+} ions are bridging two phosphate groups from the opposite strands. The binding pattern is shown in Figure 3d: three coordinated water molecules of Mg^{2+} form hydrogen bonds with O1P and O2P of phosphate groups from two strands, which facilitates a very stable binding. This implies that the distance between the phosphate backbone from the two strands is smaller than that of GC-rich segments, meaning that the A-tract region should have a much narrower minor groove width (discussed below).

From the 3D density map, one can find that the distribution of ions is dependent on the DNA sequence. The ion distribution can be quantitatively described in detail by the occupancy of bound ions at each base pair (ions within a distance of 5 Å to the atoms labeled in the inset of Figure 4d are treated as major groove ions or minor groove ions). Generally, Na^+ ions do not have distinctly favored base positions. The occupancy percentages of the major groove (Figure 4a) are slightly larger than those of the minor groove (Figure 4b) due to the fact that the major groove is more exposed to solvent. At the A-tract region, base pairs 16−19, Na^+ shows lower occupancy, especially for the minor groove. On the contrary, the situation is different for Mg^{2+} ions. As shown in Figure 4c and d, Mg^{2+} ions selectively bind to the major groove of GC base pairs, which is consistent with the patterns found in X-ray crystal structures of divalent ion in B-DNA.[41] At the major groove of the A-tract region and the minor groove of the whole

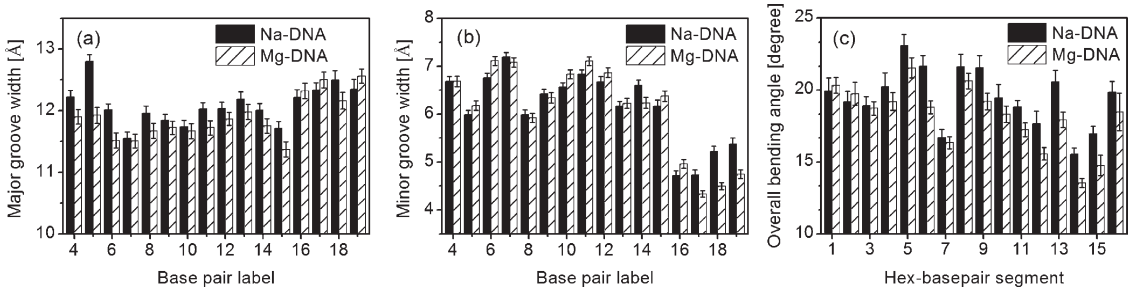

Figure 5. Major groove width (a) and minor groove width (b) of isolated DNA model. Bending angles of 16 hex-base pair segments (c). The 16 hex-base pair segments are obtained continuously from base pair 2 to 22 of the isolated DNA duplex in the study.

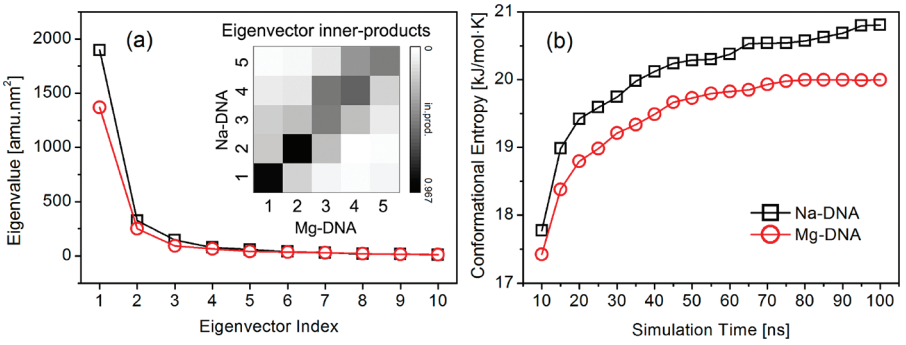

Figure 6. Eigenvalues of the first 10 eigenvectors from PCA analysis; the inset is the inner product of the first five eigenvectors from the M-DNA (*x*-axis) and N-DNA (*y*-axis) system (a). Time evolutions of conformational entropy (b).

DNA, they are almost absent. Meanwhile, only a few Na^+ ions in the Mg−DNA system can bind to DNA because Mg^{2+} ions act as strong competitors. It is interesting that in the Mg−DNA system, we also found a very low occupancy of Na^+ at the A-tract region even though Mg^{2+} ions are not present. Based on this observation, a more detailed description of ion interaction with the AT-rich DNA sequence is warranted (see discussion below). It is worth noting that the above discussions are valid without considering the terminal nucleic acids. The occupancy values of these bases may not accurately reflect their intrinsic properties because the hydrogen bonds between the terminal residues usually break, leading to high mobility of these residues.

Groove Width of DNA. The groove widths of DNA duplex are important structural characteristics which may account for the sequence-specific binding of ions. The groove width from base pair 4 to 19 was calculated with the Curves program[42] and shown in Figure 5a−b. The first three and last four base pairs were ignored because of their high mobility. We can observe that the major groove of the GC-rich segment becomes narrower while the minor groove becomes wider comparing NaCl electrolyte and $MgCl_2$ electrolytes. On the contrary, the A-tract region undergoes a reverse change: the major groove becomes wider while the minor groove becomes narrower. This difference is more obvious in the periodic-DNA model and will be discussed later.

Comparing these two segments, we find that the A-tract segment usually has a broader major groove than that of the CG-rich segment in the presence of Mg^{2+}. Thus, the absence of Mg^{2+} at the major groove of the A-tract region is not due to the steric hindrance but is an electrostatic effect. Hydrated Mg^{2+} ions interact with DNA mainly through hydrogen bond interactions which are sensitive to the environment.[41,43] As shown in Figure 4d, guanine bases can hold the hydrated Mg^{2+} ions more stably because adjacent N7 and O6 atoms can function as hydrogen bond acceptor and form hydrogen bonds simultaneously with one Mg^{2+} + $6H_2O$ complex. On the contrary, the AT base pair does not provide a good electrostatic environment for hydrated Mg^{2+}: two hydrogen acceptors, N7 atom of adenine and O4 atom of thymine, are separated by the hydrogen bond donor $-NH_2$ group on the adenine; this special configuration inhibits a Mg^{2+} + $6H_2O$ complex forming stable hydrogen bonds.

As for the minor groove (Figure 5b), it is clear that the A-tract segment has a narrower minor groove than the GC-rich region. This results in low occupancy of Na^+ (Figure 4b) and Mg^{2+} (Figure 4d) at the minor groove at base pair 16−19. Experimental data also indicated that there is no penetration of divalent ions into the spine of hydration of the minor groove.[44−46] In the simulations of the periodic-DNA model, we also observed the absence of Na^+ in the minor groove of the pAA DNA.

Structural Plasticity of DNA. Counterions are not only "passively" pulled to the vicinity of DNA and screen the electrostatic field around the polyelectrolyte, they can also "actively" modulate DNA dynamics. Analysis of the conformational entropy of DNA can be used to address this issue. First, PCA analysis was conducted in Cartesian coordinate space using the simulation trajectories. Figure 6a shows magnitudes of the 10 largest eigenvalues for the Na−DNA and Mg−DNA system. The inner products of the first five eigenvectors from the Mg−DNA and Na−DNA system are also shown in the inset. The large values of the inner products of the first two eigenvectors from the two systems ensure that the global motions of DNA molecules in these two systems are similar. Eigenvectors with large eigenvalues depict the global motion of DNA, and the quantity of the eigenvalue reflects the motion amplitude of a certain degree of freedom. We can see that the largest eigenvalue for Mg−DNA is

dx.doi.org/10.1021/jp2052568 |*J. Phys. Chem. B* 2011, 115, 14713–14720

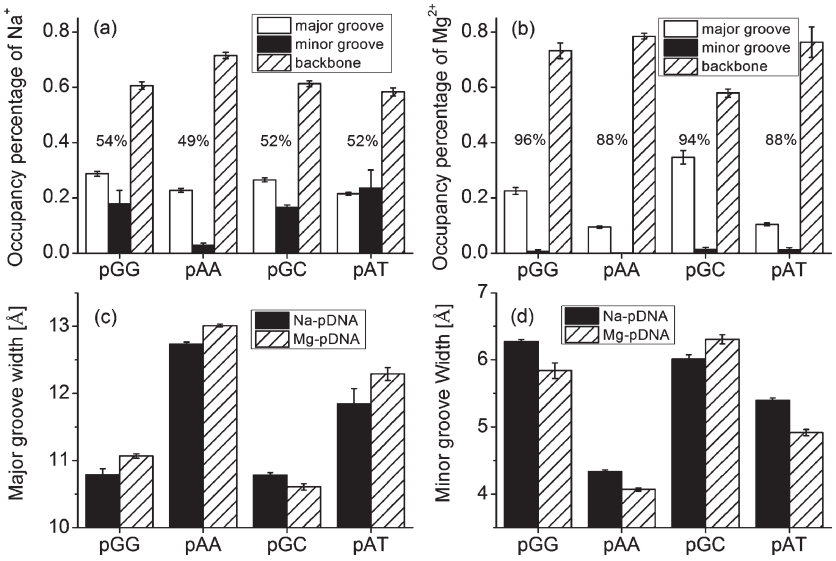

Figure 7. Base-pair-averaged number of Na^+ (a) and Mg^{2+} (b) located at major groove, minor groove, and backbone of periodic DNA. The overall charge neutralization fraction was also shown accordingly. The major groove width (c) and minor groove width (d) of periodic DNA in Na^+ and Mg^{2+} electrolytes.

smaller than that of Na−DNA, which indicates that the global motion of Mg−DNA is reduced, compared with that of Na−DNA.

The conformational entropy is computed based on the quasi-harmonic approximation that each eigenvector can be represented by a harmonic oscillator, so that the conformational entropy is calculated as[47]

$$S = k \sum_{i}^{3n-6} \frac{\hbar\omega_i/kT}{e^{\hbar\omega_i/kT} - 1} - \ln(1 - e^{-\hbar\omega_i/kT})$$

where T is the temperature and k is the Boltzmann constant; ω is the quasi-harmonic frequency which can be calculated from the eigenvalues λ obtained from the PCA analysis: $\omega_i = ((kT)/\lambda_i)^{1/2}$. The configuration entropy was calculated at a time step of 5 ns and is shown in Figure 6b. It is found that the entropy of Mg−DNA is always ~800 J/(mol·K) smaller than that of the Na−DNA system. After checking the virtual trajectory of the first eigenvector, we found that this corresponds to the global bending of the whole DNA molecule. Clearly the binding of Mg^{2+} on DNA makes it more rigid compared to that of Na^+.

The rigidity of DNA can also be represented by the local bending angles calculated using Madbend.[48] To get the local bending angles, a six-base-pair window was used to scan the whole DNA strands, resulting in 16 six-base-pair overlapping segments (ignoring the first and last base pairs). The average bending angles and error estimations are shown in Figure 5c. It was found that the local bending is reduced in the presence of Mg^{2+} ions compared to Na^+, except for the first two segments. This reflects that the bending motion of the DNA duplex is partly frozen in the presence of Mg^{2+}.

C. Results of Periodic DNA Model. Our simulation results based on an isolated 23mer DNA with an A-tract sequence have disclosed the specific Mg^{2+} ions binding and the related sequence-dependent structural and dynamical properties of DNA. In the following section we aim to confirm the above findings by employing a model of 10mer periodic DNAs with specific sequences. The periodic DNAs (pDNA) do not have tangling ending residues, and the 10 nucleic acids can be treated uniformly during the data analysis.

Ions around Periodic DNA. The average numbers of ions located nearby the DNA major/minor grooves and phosphate groups are shown in Figure 7a and b. For the Na−pDNA system, there were around 0.2−0.3 Na^+ at the major groove of the four pDNAs. Nearby the minor groove of pGG, pGC, and pAT, there were around 0.2 Na^+ ions. The most significant observation is that there was almost no Na^+ (0.028 per base) at the minor groove of pAA. This phenomenon is consistent with values in Figure 4a and b where the A-tract region has low occupancy percentage of Na^+ at major and especially minor groove. However, there is around 0.1 more Na^+ at the backbone of pAA compared to other three types of pDNA. This implies that the minor groove of pAA is very narrow. Thus Na^+ ions accumulate at the backbone without penetrating into the minor groove.

For Mg^{2+}, in the major groove, the occupancy order is the following: pGC > pGG > pAT ≈ pAA. The base-pair-averaged value of ~0.1 indicates only one Mg^{2+} exists at the major groove of pAA and pAT decamers. For pGC, the base-pair-averaged value is above 0.3, which means that there is on the average one Mg^{2+} shared by three base pairs in the major groove. In contrast, the occupancy percentage at the backbone of pGC was lower than the other three periodic DNA models. Moreover, there were almost no Mg^{2+} ions at the minor groove of four periodic DNAs, which is consistent with the isolated DNA model.

As shown in Figure 7a, although the Na^+ ions concentration increased from 0.08 M in the isolated DNA model to as high as >0.15 M in the four periodic DNA models, the neutralization fraction is still around 50% for all periodic DNAs. Experimental evidence shows that DNA condensation occurs when about 90% of its charge is neutralized by counterions.[5] Structurally, it seems that one DNA base pair can attract one Na^+ at most, so that it is impossible for DNA condensation in Na^+ electrolyte even at very high concentration. On the contrary, Mg^{2+} at 0.15−0.20 M successfully neutralized ~90% of the negative charges of DNA in the four cases as shown in Figure 7b, which may induce DNA condensation. It is interesting to see that pGG and pGC have

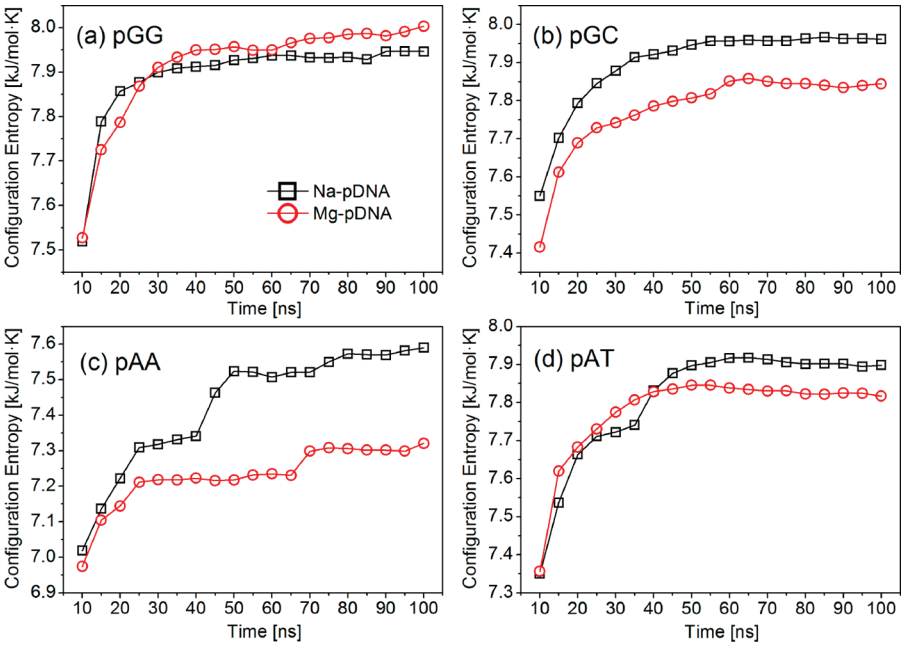

Figure 8. Time evolutions of conformational entropy of four periodic-DNA in Na^+ and Mg^{2+} electrolytes.

higher neutralization fraction values of 96% and 94% compared to those of pAA and pAT, which are 88%. This indicates that more Mg^{2+} accumulate around G·C than A·T nucleic acids which is consistent with experimental measurements on the dehydration of DNA in Mg^{2+} electrolyte, where lower dehydration effect is observed when the A·T content becomes higher.[43]

Groove Width of pDNA. As shown in Figure 7c and d, generally, pGG and pGC have narrower major grooves and broader minor grooves than AT-rich DNAs in the presence of Na^+ or Mg^{2+}. Among these four kinds of pDNA models, pGC shows distinctive structural change in the two types of electrolytes: the major groove of pGC in Na^+ is broader than that in Mg^{2+}, while the minor groove of pGC in Na^+ is narrower than that in Mg^{2+}. It may also be noted that pAA has the narrowest minor groove (~4 Å), which facilitates the very stable Mg^{2+} binding on the phosphate as shown in Figure 3d. This also explains the reason that there are almost no ions at the minor groove of pAA.

Conformational Entropy of pDNA. Finally we studied the conformational entropy in periodic-DNA system under the influence of the counterions. As shown in Figure 8, we can see that Mg^{2+} ions exert "freezing" effects on DNA dynamics compared with Na^+ ions for pGC, pAA, and pAT DNAs. For pGG DNA, the freezing effects are not evident. The conformational entropies in Mg^{2+} and Na^+ do not differ too much (the largest difference is for pAA, around 0.3 kJ/(mol·K) per 10 base pairs). The main reason is that in the periodic systems the DNA decamer is covalently bonded to its image, and the overall bending in this DNA model is totally inhibited. The conformational entropy of the periodic DNAs may mainly capture local motions like base pair tilt, roll, and twist, etc.

4. CONCLUSION

In brief, molecular dynamics simulations of DNA duplex in the presence of Mg^{2+} and Na^+ ions were performed. Na^+ ions have less stable hydration shell and interact with DNA nonspecifically. On the contrary, Mg^{2+} ions have stable hydration shell and interact with DNA mainly through hydrogen bonds. Thus, Mg^{2+} ion binding is sensitive to the local environment and is sequence-specific. Although A·T nucleic acids are found to have broader major groove than G·C nucleic acids, Mg^{2+} ions were only found in the major groove of the G·C base pairs. This binding selectivity has an electrostatic nature and is not of steric origin. The adjacent N7 and O6 atoms at guanine base create a negative potential environment and act as hydrogen bond acceptor for hydrated Mg^{2+} ions, while the positively charged H atoms on the N6 amino group of adenine base repel the hydrated cations. Moreover, the binding of Mg^{2+} ions make the DNA duplex more rigid. The overall conformational entropy of Mg^{2+}-bound DNA is significantly less than that of Na^+-bound DNA, and the local bending amplitudes are also reduced in the presence of Mg^{2+} ions. We expect that the sequence-specific binding of Mg^{2+} will lead to distinct DNA condensation patterns in the context of different DNA sequences.

AUTHOR INFORMATION

Corresponding Author
*E-mail: ygmu@ntu.edu.sg.

ACKNOWLEDGMENT

The computational resources support by IDA Cloud Computing Call for Project Proposals 2010 is gratefully acknowledged.

REFERENCES

(1) Saenger, W. *Principles of Nucleic Acid Structure*; Springer: New York, 1984.
(2) Sharp, K. A.; Honig, B. *Curr. Opin. Struct. Biol.* **1995**, *5*, 323.
(3) Draper, D. E. *RNA* **2004**, *10*, 335.
(4) Woodson, S. A. *Curr. Opin. Chem. Biol.* **2005**, *9*, 104.
(5) Victor, A. B. *Biopolymers* **1997**, *44*, 269.
(6) McFail-Isom, L.; Hu, G. G.; Williams, L. D. *Biochemistry* **1998**, *37*, 8341.

(7) Sines, C. C.; McFail-Isom, L.; VanDerveer, D.; Williams, L. D. *Biochemistry* **1998**, *37*, 16877.
(8) Serra, M. J.; Baird, J. D.; Dale, T.; Fey, B. L.; Retatagos, K.; Westhof, E. *RNA* **2002**, *8*, 307.
(9) Kankia, B. I. *Biophys. Chem.* **2003**, *104*, 643.
(10) Sosnick, T. R.; Pan, T. *Curr. Opin. Struct. Biol.* **2003**, *13*, 309.
(11) Woodcock, C. L.; Dimitrov, S. *Curr. Opin. Genet. Dev.* **2001**, *11*, 130.
(12) Dixit, S. B.; Beveridge, D. L.; Case, D. A.; Cheatham, T. E.; Giudice, E.; Lankas, F.; Lavery, R.; Maddocks, J. H.; Osman, R.; Sklenar, H.; Thayer, K. M.; Varnai, P. *Biophys. J.* **2005**, *89*, 3721.
(13) Varnai, P.; Zakrzewska, K. *Nucleic Acids Res.* **2004**, *32*, 4269.
(14) Auffinger, P.; Hashem, Y. *Curr. Opin. Struct. Biol.* **2007**, *17*, 325.
(15) Ponomarev, S. Y.; Thayer, K. M.; Beveridge, D. L. *Proc. Natl. Acad. Sci. U.S.A.* **2004**, *101*, 14771.
(16) Várnai, P.; Timsit, Y. *Nucleic Acids Res.* **2010**, *38*, 4163.
(17) Denisov, V. P.; Halle, B. *Proc. Natl. Acad. Sci. U.S.A.* **2000**, *97*, 629.
(18) Cheatham, T. E. *Curr. Opin. Struct. Biol.* **2004**, *14*, 360.
(19) Rueda, M.; Cubero, E.; Laughton, C. A.; Orozco, M. *Biophys. J.* **2004**, *87*, 800.
(20) Varnai, P.; Zakrzewska, K. *Nucleic Acids Res.* **2004**, *32*, 4269.
(21) Hamelberg, D.; Williams, L. D.; Wilson, W. D. *J. Am. Chem. Soc.* **2001**, *123*, 7745.
(22) Luan, B.; Aksimentiev, A. *J. Am. Chem. Soc.* **2008**, *130*, 15754.
(23) Duguid, J.; Bloomfield, V. A.; Benevides, J.; Thomas, G. J. *Biophys. J.* **1993**, *65*, 1916.
(24) Colmenarejo, G.; Tinoco, I., Jr. *J. Mol. Biol.* **1999**, *290*, 119.
(25) Misra, V. K.; Draper, D. E. *Proc. Natl. Acad. Sci. U.S.A.* **2001**, *98*, 12456.
(26) Strauss, J. K.; Maher, L. J., III. *Science* **1994**, *266*, 1829.
(27) Prabhu, N. V.; Panda, M.; Yang, Q.; Sharp, K. A. *J. Comput. Chem.* **2008**, *29*, 1113.
(28) Pérez, A.; Marchán, I.; Svozil, D.; Sponer, J.; Cheatham, T. E.; Laughton, C. A.; Orozco, M. *Biophys. J.* **2007**, *92*, 3817.
(29) Macke Thomas, J.; Case David, A. Modeling Unusual Nucleic Acid Structures. In *Molecular Modeling of Nucleic Acids*; American Chemical Society: Washington, DC, 1997; Vol. 682, pp 379.
(30) MacKerell, A. D.; Bashford, D.; Bellott; Dunbrack, R. L.; Evanseck, J. D.; Field, M. J.; Fischer, S.; Gao, J.; Guo, H.; Ha, S. *J. Phys. Chem. B* **1998**, *102*, 3586.
(31) Jorgensen, W. J.; Chandrasekhar, J.; Madura, J. D.; Impey, R. W.; Klein, M. L. *J. Chem. Phys.* **1983**, *79*, 926.
(32) David Van Der, S.; Erik, L.; Berk, H.; Gerrit, G.; Alan, E. M.; Herman, J. C. B. *J. Comput. Chem.* **2005**, *26*, 1701.
(33) Ryckaert, J. P.; Ciccotti, G.; Berendsen, H. J. C. *J. Comput. Phys.* **1977**, *23*, 327.
(34) Essmann, U.; Perera, L.; Berkowitz, M. L.; Darden, T.; Lee, H.; Pedersen, L. G. *J. Chem. Phys.* **1995**, *103*, 8577.
(35) Darden, T.; Perera, L.; Li, L.; Pedersen, L. *Structure* **1999**, *7*, R55.
(36) Toshiko, I.; Martin, K. *Proteins: Struct., Funct., Genet.* **1991**, *11*, 205.
(37) Schlitter, J. *Chem. Phys. Lett.* **1993**, *215*, 617.
(38) Subirana, J. A.; Soler-López, M. *Annu. Rev. Biophys. Biomol. Struct.* **2003**, *32*, 27.
(39) Bleuzen, A.; Pittet, P.-A.; Helm, L.; Merbach, A. E. *Magn. Reson. Chem.* **1997**, *35*, 765.
(40) Joung, I. S.; Cheatham, T. E. *J. Phys. Chem. B* **2008**, *112*, 9020.
(41) Chiu, T. K.; Dickerson, R. E. *J. Mol. Biol.* **2000**, *301*, 915.
(42) Stofer, E.; Lavery, R. *Biopolymers* **1994**, *34*, 337.
(43) Buckin, V. A.; Kankiya, B. I.; Rentzeperis, D.; Marky, L. A. *J. Am. Chem. Soc.* **1994**, *116*, 9423.
(44) Haran, T. E.; Mohanty, U. *Q. Rev. Biophys.* **2009**, *42*, 41.
(45) Minasov, G.; Tereshko, V.; Egli, M. *J. Mol. Biol.* **1999**, *291*, 83.
(46) Soler-Lopez, M.; Malinina, L.; Liu, J.; Huynh-Dinh, T.; Subirana, J. A. *J. Biol. Chem.* **1999**, *274*, 23683.
(47) Andricioaei, I.; Karplus, M. *J. Chem. Phys.* **2001**, *115*, 6289.
(48) Strahs, D.; Schlick, T. *J. Mol. Biol.* **2000**, *301*, 643.